Characterizing temporal changes in forest fire ignitions: looking for climate change signals in a region of the Canadian boreal forest

Douglas G. Woolford, Jiguo Cao, Charmaine B. Dean and David L. Martell

Douglas G. Woolford (*Corresponding Author*)
Wilfrid Laurier University
Mathematics
75 University Avenue West
Waterloo, ON, CAN N2L 3C5
Tel: (819) 884-0710 Ext. 2296
Fax: (519) 884-9738
E-Mail: dwoolford@wlu.ca

Jiguo Cao
Simon Fraser University
Statistics and Actuarial Science
8888 University Drive
Burnaby, BC, CAN V5A 1S6
E-Mail: jiguo_cao@sfu.ca

Charmaine B. Dean
Simon Fraser University
Statistics and Actuarial Science
8888 University Drive
Burnaby, CAN V5A 1S6
E-Mail: dean@stat.sfu.ca

David L. Martell
University of Toronto
Faculty of Forestry
Earth Sciences Centre
33 Willcocks Street
Toronto ON, CAN M5S 3B3
E-Mail: martell@smokey.forestry.utoronto.ca

Characterizing temporal changes in forest fire ignitions: looking for climate change signals in a region of the Canadian boreal forest

Douglas G. Woolford[1], Jiguo Cao[2], Charmaine B. Dean[2] and David L. Martell[3]

Abstract

The potential impact of climate change on forest fire risk is of significant concern. Postulated climate change effects on wildfires include increasing annual trends in ignitions and a lengthening of the fire season. We propose to use logistic generalized additive mixed models to investigate these characteristics. We present the modelling framework and outline a set of candidate models that are nested in terms of their fixed effects components. Model selection via likelihood ratio testing is discussed and connected to an entropy-based scoring rule for Bernoulli responses. We illustrate its application using data for lightning-caused forest fire ignitions over a period of 42 years in a 9,884,943 hectare region of boreal forest of northwestern Ontario, Canada. Seasonal and annual changes in ignition risk are observed and discussed, but we identify significant outstanding confounding factors that need to be addressed before one can assess the extent to which those changes can or cannot be attributed to climate change.

Keywords: entropy score, generalized additive mixed model, nonparametric smoothing, wildfire ignitions

[1]Department of Mathematics; Wilfrid Laurier University; Waterloo, Canada N2L 3C5
[2]Department of Statistics and Actuarial Science; Simon Fraser University; Burnaby, Canada V5A 1S6
[3]Faculty of Forestry; University of Toronto; Toronto, Canada M5S 3B3

1 Introduction

The management of Canada's boreal forest is a challenging task due in part to the long planning horizons associated with renewable forest resources. Forest management agencies use planning models to make decisions related to budgeting, forecasting and resource allocation. Hence, identifying and incorporating changes to forest fire regime characteristics is a key component to forest management. In addition, uncertainty concerning the extent to which climate change has the potential to impart changes to forest fire regimes has become a significant concern in Canada.

The motivation for investigating climate change trends and their potential impacts on forest fire risks has been fuelled by extreme and high-profile events, such as the many fires that burned across the southern interior of the province of British Columbia in 2003, including the Okanagan Mountain Park forest fire that burned parts of the city of Kelowna. That fire spread to roughly 25,000 hectares in size and accrued approximately 400 million ($CAD) in suppression costs. It was one of many fires that occurred during that summer, which was one of the driest summers on record. (Filmon, 2004). Extreme weather events such as this are of immediate concern, because weather is widely accepted as being the primary factor that drives forest fire behaviour.

A study to characterize the distribution of dry-spell extremes and extreme fire sizes was performed by Beverly and Martell (2005). There, they found the distribution of these events differed for the western and eastern boreal shield ecozones in Ontario, Canada. Climate change studies assessing the impact of a warming climate using forecasts from general circulation models have suggested increased seasonal severity ratings and monthly area burned for Canada (Flannigan and Van Wagner, 1991; Flannigan et al., 2005), along with an increase in human-caused forest fire ignitions in Ontario (Wotton et al., 2003). Quality-control methodology, applied by Podur et al. (2002), found a change in variability associated with fire occurrence and area burned by forest fires over two different time periods for three study areas in regions of Canada. Weber and Stocks (1998) proposed that increases in temperature could potentially alter a fire regime in three ways: an increase in severe fire weather, an increase in ignitions and an extended fire season. This paper presents a method that can be employed for initial exploration of the latter two effects.

We investigate annual trends and changes in fire season lengths using logistic generalized ad-

ditive mixed models. We outline a set of nested candidate models whose fixed effects include seasonality components, annual trends and their interactions as partial effects, and discuss model selection. An annual random effect is incorporated to account for year-to-year variability, while serial autocorrelation within the fire season is accounted for via an AR(1) component.

The general modelling framework, the candidate models, and a discussion on model selection with a connection to an entropy-based scoring rule for Bernoulli responses is presented in Section 2. Using this framework, we explore for potential climate change effects in lightning-caused forest fire ignitions for a region of boreal forest in northwestern Ontario, Canada in Section 3. Section 4 concludes the paper with a discussion of the analysis and extensions for future work.

2 A Generalized Additive Mixed Model Framework

Let the univariate response of interest be denoted by the random variable Y_i and assume that, conditional on random effects, its distribution belongs to the exponential family. A generalized additive mixed model (GAMM) has the following general structure

$$g\big(\mathrm{E}(Y_i)\big) = \sum_{j=1}^{r} f_j(x_{ji}) + \mathbf{X}_i\boldsymbol{\beta} + \mathbf{Z}_i\mathbf{b} + \epsilon_i \ , \tag{1}$$

where $g(\cdot)$ denotes the "link function" (see, e.g., McCullagh and Nelder, 1989); the $f_j(\cdot)$ are smooth functions of the covariates x_j; $\mathbf{X}_i$ is the i^{th} row of the design matrix for the fixed effects, whose p coefficients are contained in the vector $\boldsymbol{\beta}$; $\mathbf{Z}_i$ is the i^{th} row of the design matrix for the random effects, whose q coefficients are contained in the vector $\mathbf{b}$. This vector of random effect coefficients is assumed to be normally distributed with zero mean and covariance matrix $\boldsymbol{\psi}$, and it is also assumed to be independent of the vector of residual errors, consisting of the elements ϵ_i, which have zero mean and covariance matrix Λ.

The structure of the data will dictate the random effects components. For example, in the analysis of our data, correlation between sequential observations within each fire season and year-to-year variability needs to be accounted for, which motivates the specific structure of the model for forest fire ignitions we now describe.

2.1 Logistic GAMMs for Forest Fire Ignitions

We define a *fire day* as a day during which one or more fires are reported in a designated area. Let $p(t_{dy})$ denote the probability of a fire on day d of year y. To investigate for climate change effects, such as inter-annual trends or changes to the duration of the fire season, we model this probability using GAMMs of the form

$$\text{logit}\big(p(t_{dy})\big) = \beta_0 + f(d, y) + \epsilon_y + e_{dy}$$

where β_0 is an intercept, and the other fixed effect, $f(d, y)$, is a nonparametric smooth function of time without intercept. The remaining two components are random: year-to-year differences in overall ignition risk are modelled via the annual random effect term ϵ_y, while within-year serial autocorrelation is accounted for using the AR(1) process $e_{dy} = \phi e_{(d-1)y} + \epsilon_{dy}$. Here, ϵ_y and ϵ_{dy} are mutually independent normally distributed random variables, each with a mean of zero and variances of σ_y^2 and σ_{dy}^2, respectively.

The presence of seasonal behaviour, annual trends, and their interaction can be investigated by comparing models where the fixed effect $f(d, y)$ takes on the following forms:

$$\begin{aligned}
\text{M}_0: &\quad f(d, y) = 0\ , \\
\text{M}_1: &\quad f(d, y) = f_1(d)\,, \\
\text{M}_2: &\quad f(d, y) = f_2(d) + f_3(y)\ \text{, or} \\
\text{M}_3: &\quad f(d, y) = f_4(d, y)\ .
\end{aligned}$$

The null model M_0 assumes the same ignition risk every day of the fire season for of every year; model M_1 indicates that the same seasonality trend is present across all years; model M_2 allows an additive annual trend effect to translate a non-changing seasonality effect; and, model M_3 incorporates an additional interaction term that allows for different seasonal effects across years. Note that M_2 is conceptually, but not explicitly nested within the bivariate smooth function in M_3. Hence, caution is warranted in the use of likelihood ratio tests for comparing these models. We elaborate on this point later on in this section.

The smooth functions in the above models are represented using linear combinations of basis functions. For example, the univariate smooths in M_2 can be represented as

$$f_2(d) = \sum_{k=1}^{K} b_k \phi_k(d) \ , \quad \text{and} \quad f_3(y) = \sum_{l=1}^{L} c_l \psi_l(y) \, ,$$

where b_k and c_l are unknown parameters to be estimated, and $\phi_k()$ and $\psi_l()$ are piecewise polynomials, namely cubic regression splines, which are joined at the set of "knots" that index the above summations and represent a partition of the range of the corresponding covariate effect being modelled. The bivariate smoother in M_3 is constructed similarly, except the unknown parameter in the basis function expansion is allowed to vary in both directions. That is,

$$f_4(d, y) = \sum_{k=1}^{K} \sum_{l=1}^{L} d_{kl} \phi_k(d) \psi_l(y)$$

The number of knots, K and L, for such systems are chosen by minimizing the respective generalized cross-validations (Gu, 2002). All basis coefficients are estimated by maximizing a penalized likelihood function, where the penalty terms control the amount of smoothing. For example, if $l(\boldsymbol{\theta})$ denotes the log-likelihood for a GAMM parameterized by $\boldsymbol{\theta}$, then a corresponding penalized log-likelihood is given by

$$l(\boldsymbol{\theta}) - \sum_{j=1}^{r} \lambda_j \int \left[f_j''(x_j) \right]^2 dx_j$$

where $f_j''(x_j)$ denotes the second derivative of the jth smooth term in the model. In other words, the total roughness in f_j is penalized by a factor of λ_j, a parameter controlling the tradeoff between the total "wiggliness" of that smoother and how it fits the data. These penalty parameters are chose to minimize the Generalized Cross Validation score (Craven and Wahba, 1979; Golub et al., 1979). Further technical details on modelling and GCV estimation for generalized additive models with multiple smoothing parameters appear in Wood (2000, 2004, 2006).

2.2 Model selection and a connection to entropy-based scoring rules in models for Bernoulli responses

When fitting these types of models, a common method employed to test for goodness of fit is to use the deviance. As described by Dobson (2002), the deviance is equal to twice the log-likelihood ratio statistic of the fitted model relative to a saturated model (a corresponding model fitted with the maximum number of parameters). For a model fitted with p parameters and a corresponding saturated model with $m > p$ parameters, the sampling distribution of the deviance is approximately Chi-Squared with $m - p$ degrees of freedom. In addition, differences in deviance can be used to compare the fit between two nested models via a generalized likelihood ratio test. That is, one can test the null hypothesis that there is no difference between a linear model with q parameters, whose linear component is a subset of a more general model, which has $p > q$ parameters. To do so, one examines the difference in the observed deviances for the two nested models being compared. For example, the likelihood ratio test statistic for comparing models with the fixed effect specified by M_2 to that specified by M_1 (i.e., a test for the presence of an annual trend effect) is based on

$$\lambda = 2[l(\mathbf{y}|M_2) - l(\mathbf{y}|M_1)]\,,$$

where $l(\mathbf{y}|M_d)$, $d = 0, 1, 2, 3$, is the log-likelihood function under the model M_d. Under the null, λ follows a χ^2 distribution with degrees of freedom given by the difference in the number of parameters between two models. Wood (2006) noted this is true in general if each smooth term in the estimated null model has no more basis functions than the same term in the alternative model.

We also remark that there is a direct connection between this analysis of deviance test for comparing goodness of fit to observed data, and an entropy-based scoring method for assessing a model's "goodness of prediction" on future observations. Daley & Vere-Jones (2003, pp 276-278) note for a single observation with a "good" (i.e., close to the true value) forecast probability, the expectation of the binomial score corresponds to the entropy score. Furthermore, by summing the entropy score over a set of estimated forecast probabilities one obtains the log-likelihood of the model. Hence, maximizing the entropy score corresponds to testing the predictive fit of a model

based on its likelihood. Since the case where all points in a set of n independent Bernoulli trials are assumed to have equal success probability of $1/n$ (i.e., the discrete Uniform) is the hardest distribution to predict when using a binomial score, Daley & Vere-Jones (2003) suggest using it as a reference distribution. This results in the entropy score representing the "expected information gain" or, in other words "the improvement in the predictability of the model used, relative to the reference model". Hence, using the discrete Uniform distribution as the reference distribution in such an entropy score provides a method for comparing prediction efficiency between models.

Consider a process consisting of independent Bernoulli trials Y_i. Denote the probability of success for the ith trial by $p_i = \Pr\{Y_i = 1\}$. For a realization of n trials $\mathbf{Y} = (Y_1, \ldots, Y_n)$, with corresponding success probabilities $\mathbf{p}_1 = (p_1, \ldots, p_n)$, the log-likelihood is given by

$$\log\, L(\mathbf{Y}; \mathbf{p}_1) = \sum_{i=1}^{n} \{Y_i \log(p_i) + (1 - Y_i)\log(1 - p_i)\} \tag{2}$$

Following the same notation, and denoting the discrete Uniform reference distribution probabilities as $\mathbf{p}_2 = \{1/n,\ \ldots,\ 1/n\}$, the entropy measure for a Bernoulli process with n observations on the interval $[0,\ T]$ can be expressed as

$$\log\, \frac{L(\mathbf{Y};\ \mathbf{p}_1)}{L(\mathbf{Y};\ \mathbf{p}_2)} = \sum_{i=1}^{n} \left[Y_i \log\left(\frac{p_i}{1/n}\right) + (1 - Y_i)\log\left(\frac{1 - p_i}{1 - 1/n}\right)\right] \tag{3}$$

This difference in entropy between two models is, in fact, the analysis of deviance test we employ.

It is important to note that there are some additional approximations underlying the use of such a test in the context of additive models where smooth fixed effects are modelled via penalized splines. Specifically: (i) the test uses the penalized fits with effective degrees of freedom found by evaluating the trace of a penalized "hat" matrix, not un-penalized fits with known degrees of freedom; (ii) smoothing parameters were estimated to fit the model, and thus, the test is conditional on these parameters; and, (iii) the additive representation of marginal smooths $f_2(d) + f_3(y)$ is conceptually, but not explicitly, nested within the bivariate smooth $f_3(d, y)$. Wood (2006) identified these caveats, and noted that one should take care if there is not a "clear-cut" rejection of one model in favour of an alternative. However, as we demonstrate in the next section, this does not turn out to be the case for the models we build and compare.

3 Exploring lightning-caused forest fire ignitions in a region of Canada's boreal forest.

In this section we illustrate the use of the methodology described above by performing an exploratory analysis of forest fire ignitions in a section of Canada's boreal forest, focusing on looking for possible climate change signals. Our data consist of records of all detected lightning-caused forest fires that occurred during Ontario's official fire season (April 1 through October 31 of each year; the climate in the late fall through the end of winter is this region is not conducive to the ignition of forest fires) for the years 1963 through 2004 in a region of northwestern Ontario's boreal forest. Our 3,371,186 hectare study area consists of the Lake of The Woods (Ontario portion only) and Rainy River *ecoregions*–area that are relatively homogeneous with respect to their climate, vegetation, geography and other ecological characteristics (Ecological Stratification Working Group, 1995). There were 1,259 fire days in this region during this period. Figure 1 plots the observed proportion of fire days by day of year (panel a) and by year (panel b). It is clear that there is a strong seasonal trend within each year, while there can also be considerable variability between years. Hence, the fixed and random effect components in the models we outline in Section 2.1 appear reasonable.

Data were provided by Aviation, Forest Fire and Emergency Services of the Ontario Ministry of Natural Resources (OMNR), which is responsible for the detection and suppression of forest fires, along with fire prevention, prescribed burning and other forest management activities on all Crown land in Ontario's fire region. Historically, their fire management strategy in our study area has been to actively suppress all forest fires. Although this area is actively managed, there is the potential for changes in organized and unorganized detection patterns. In the last section of this paper we discuss such confounders and implications for interpreting the results of the analysis.

3.1 Model Selection and Estimated Effects

We first fit the four models described in Section 2.1 to our sample data set. Model selection via likelihood ratio tests (Table 1) indicate the model with a bivariate smoother of day of year and of year (i.e., M_3) is preferred. Figure 2 visualizes the fitted probabilities obtained from this model

against time as a three-dimensional smooth surface, while Figure 3 illustrates the corresponding contours of this surface. Each plot is colour-coded to emphasize the estimated changes in fire ignition risk. As expected, the seasonal nature of forest fire ignitions is evident: the ignition risk is zero during the late fall through early spring and then it increases, peaking in the early summer, while there is an overall increasing trend in ignition risk across years. Moreover, the heterogeneity of the surface across years suggests 1) that, at the peak of the fire season, the risk of lightning ignitions has generally increased over the study period, and 2) that the start, the end, and the length of the fire season has not remained constant over time. For example, consider the two 10% contours in Figure 3. Tracking these over time, we see that in the first half of the fire season (i.e., the bottom 10% contour) this risk level appears to fluctuate around the same day of the year: in 1963 the bottom 10% contour occurs at day 161, while in 2004 it is at day 159. However, there seems to be a more prominent shift in this risk level towards later on in the fire season each year: in 1963 the top 10% contour is day 247, while in 2004 it is at day 259. Similar patterns are observed in the neighbouring 5% and 15% contours.

A commonly employed technique to assess the goodness of fit of a logistic model is to compare the observed number of events to those expected under the model. The latter quantity is readily obtained by first transforming the model's fitted values to the response scale via the inverse logit function, and then summing these fitted probabilities over any period of interest. Based on such a comparison, the obtained model appears to fit quite well: our model expected 1,160 fire days and 1,259 such days were observed in the data set. The observed and expected values are quite close when aggregated weekly over all years (Figure 4, panel a). When counts are aggregated on an annual basis (panel b) the year-to-year variability in observed counts is very apparent.

The estimated parameter for the AR(1) component was $\hat{\phi} = 0.254$, and the variance for the autoregressive component was estimated to be $\hat{\epsilon}_{dy} = 0.667$. The annual random effect was estimated to have a variance of $\hat{\epsilon}_{y} = 0.469$. The latter variance component captures the inter-annual variability in the data quite well (5). When the posterior estimates (see Brillinger et al., 2006) of the each year's random effect (panel a) are added back to the respective fitted values for each year and pseudo-probabilities are then calculated, the resulting pseudo-expected number of fire days each year come very close to matching the observed counts (panel b).

4 Discussion

The purpose of this study was to investigate the extent to which there has or has not been a change in the length and other features of the fire season in northwestern Ontario. We focused on model selection procedures for a set of candidate logistic generalized additive mixed models, where the fixed effects components were nested in such a way that seasonal trends, inter-annual trends, and their potential interaction could be investigated. Such a framework permitted us to explore for two important possible climate change effects: annual increases in fire ignition risk and changes to the duration of the fire season. A random effect component was included to account for year-to-year variability, and serial autocorrelation within each year's set of observations was modelled via an AR(1) process.

We illustrated the application of this framework on a sample of lightning ignition data for a boreal region in northwestern Ontario. Our results suggest that both ignition risk (the probability of a fire day) and the number of weeks that this risk is nonzero (the effective length of the fire season) have been changing over time. We found that a model with a fixed effect that was a bivariate smoother of day of year and year fit the data best, in terms of both the Chi-squared-based hypothesis testing, and visual assessments of goodness of fit which compared observed versus expected counts aggregated on different temporal scales. When comparing annually aggregated counts the need for the annual random effect was very clear. When posterior estimates of these annual random effects were used to create fitted pseudo probabilities there was a dramatic improvement in fit (Figure 5). This corroborates previous findings by Brillinger et al. (2006), who concluded that an annual random effect was a crucial component given the context of the problem and the need for predictive forecasts. Their analysis focused on estimating wildfire ignition risk in Oregon and California, and analyzed data on a very fine spatio-temporal scale. The identification of a changing fire season is also of importance. For example, Westerling et al. (2006) showed that the frequency of large-area wildfires in the western United States was associated with not-only increased fire season temperatures, but an earlier spring snowmelt.

Although our findings are consistent with predictions that climate change may result in increases in both lightning fire occurrence and the length of the fire season (Flannigan and Van Wagner,

1991) it is important to note that our results may be due to climate change and/or changes in fire detection effectiveness. To assess whether our observed signal may be caused or influenced by detection effectiveness, we carried out a simple exploratory analysis of size at detection, which can be viewed as a surrogate measure of detection system effectiveness. Annual boxplots of the logarithm of the estimated size at detection for all lightning ignited fires in this study region (Figure 6) suggest larger sizes for approximately the first half of the study period. Lightning-caused fires can occur in more remote areas, and may take longer to detect than people-caused fires. These fires would continue to grow until detected. The fact that the size at detection appears to be higher in earlier years suggests that detection system performance may have improved in this study area over time. Hence, the increase in fire activity that we are observing may be due to climate change, or improved detection system performance, or some combination of both of these factors.

Besides investigating the source of the observed signals, further work involves extensions to permit the joint analysis of several ecoregions by allowing the coefficients of the spline smoothers as well as the probabilities of extreme events to very smoothly over space. This will provide a broad framework for the spatio-temporal investigations into intra and inter-annual trends, and their interactions, for a variety of discrete and continuous outcomes.

5 Acknowledgements

The authors gratefully acknowledge the support of Geomatics for Informed Decisions (GEOIDE SII Project 51), the National Institute for Complex Data Structures and the Natural Sciences and Engineering Research Council of Canada. We thank the Ontario Ministry of Natural Resources for the use of their data, Vivien Wong for some related exploratory analyses, and three anonymous referees for helpful comments. Computations were performed in R (R Core Development Team, 2009) using the mgcv package, version 1.5-6 (Wood, 2006).

References

[1] Beverly, J.L and Martell, D.L. 2005. Characterizing extreme fire and weather events in the Boreal Shield ecozone of Ontario. *Agricultural and Forest Meteorology*, **133**: 5-16.

[2] Brillinger, D.R., Preisler, H.K. and Benoit, J.W. 2006. Probabilistic risk assessment for wildfires. *Environmetrics*, **17**: 622–633. DOI: 10.1002/env.768.

[3] Coles, S. G. 2001. An Introduction to Statistical Modeling of Extreme Values. Springer: London.

[4] Craven, P. and Wahba, G. 1979. Smoothing noisy data with spline functions. *Numerische Mathematik* **31**: 377–403.

[5] Daley, D.J. & Vere-Jones, D. (2003). *An Introduction to the Theory of Point Processes. Volume 1: Elementary Theory and Methods, Second Edition.* Springer-Verlag: New York.

[6] Dobson, A.J. (2002). *An Introduction to Generalize Linear Models, 2nd Ed.* Chapman & Hall: New York.

[7] Ecological Stratification Working Group. 1995. A National Ecological Framework for Canada. Agriculture and Agri-Food Canada, Research Branch, Centre for Land and Biological Resources Research and Environment Canada, State of Environment Directorate, Ecozone Analysis Branch, Ottawa/Hull. Report and national map at 1:7 500 000 scale.

[8] Filmon, G. 2004. *Firestorm 2003: provincial review.* Government of British Columbia, Canada. 100p.

[9] Flannigan, M.D., Logan, K.A., Amiro, B.D., Skinner, W.R. and Stocks, B.J. 2005. Future area burned in Canada. *Climatic Change*, **72**: 1–16. DOI:10.1007/s10584-005-5935-y

[10] Flannigan, M.D. and Van Wagner, C.E. 1991. Climate change and wildfire in Canada. *Can. J. For. Res.*, **21**: 66–72.

[11] Golub, G.H., Heath, M. and Wahba, G. 1979. Generalized cross validation as a method for choosing a good ridge parameter. *Technometrics* **21(2)**: 215–223.

[12] Gu, C. 2002. Smoothing Spline ANOVA Models. Springer: New York.

[13] McCullagh, P. and Nelder, J.A. 1989. *Generalized linear models* (2nd ed.). Chapman and Hall: London, U.K.

[14] Podur, J., Martell, D.L. and Knight, K. 2002. Statistical quality control analysis of forest fire activity in Canada. *Can. J. For. Res.*, **32**: 195–205. DOI:10.1139/X01-183.

[15] R Development Core Team (2009). R: A language and environment for statistical computing. R Foundation for Statistical Computing, Vienna, Austria. ISBN 3-900051-07-0, URL http://www.R-project.org.

[16] Stocks, B. J., et al. (2002), Large forest fires in Canada, 19591997, *J. Geophys. Res.*, **107**, 8149. doi:10.1029/2001JD000484, [printed 108(D1), 2003].

[17] Weber, M.G. and Stocks, B.J. 1998. Forest fires in the boreal forests of Canada. In J.M. Moreno (ed), *Large Forest Fires*, pp. 215–233. Blackhuys Publishers, Leiden, The Netherlands.

[18] Westerling, A.L., Hidalgo, H.G., Cayan, D.R., and Swetnam, T.W. 2006. Warming and earlier spring increase Western U.S. forest wildfire activity. *Science*, **313**: 940–943.

[19] Wood, S.N. 2000. Modelling and smoothing parameter estimation with multiple quadratic penalties. *J. R. Statist. Soc. B*, **62**: 413–428.

[20] Wood, S.N. 2004. Stable and efficient multiple smoothing parameter estimation for generalized additive models. *J. Amer. Statist. Assoc.* **99(467)**: 673–686. doi:10.1198/016214504000000980.

[21] Wood, S.N. 2006. Generalized Additive Models: An Introduction with R. Chapman and Hall/CRC Press: Boca Raton, FL.

[22] Wotton, B.M., Martell, D.L. and Logan, K.A. 2003. Climate change and people-caused forest fire occurrence in Ontario. *Climatic Change*, **60**: 275–295.

Model	log-likelihood	$\lvert\Delta$log-likelihood$\rvert$	edf	$\lvert\Delta$edf $\rvert$	P-value
M_0	40642.17	NA	15329.00	NA	NA
M_1	67722.77	27080.60	15323.77	5.23	≈ 0
M_2	66593.69	1129.08	15322.68	1.09	≈ 1
M_3	75110.94	8517.25	15316.80	5.88	≈ 0

Table 1: Likelihood ratio test results: the first column is used to denote the form of the component $f(d, y)$ in the model. The log-likelihood and effective degrees of freedom (edf) for each of these candidate models appear in columns 2 and 4, respectively. The magnitude of the successive differences for the log-likelihood and the edf are then given in columns 3 and 5. The p-value for the likelihood ratio test that compares each of these successive models appears in the last column.

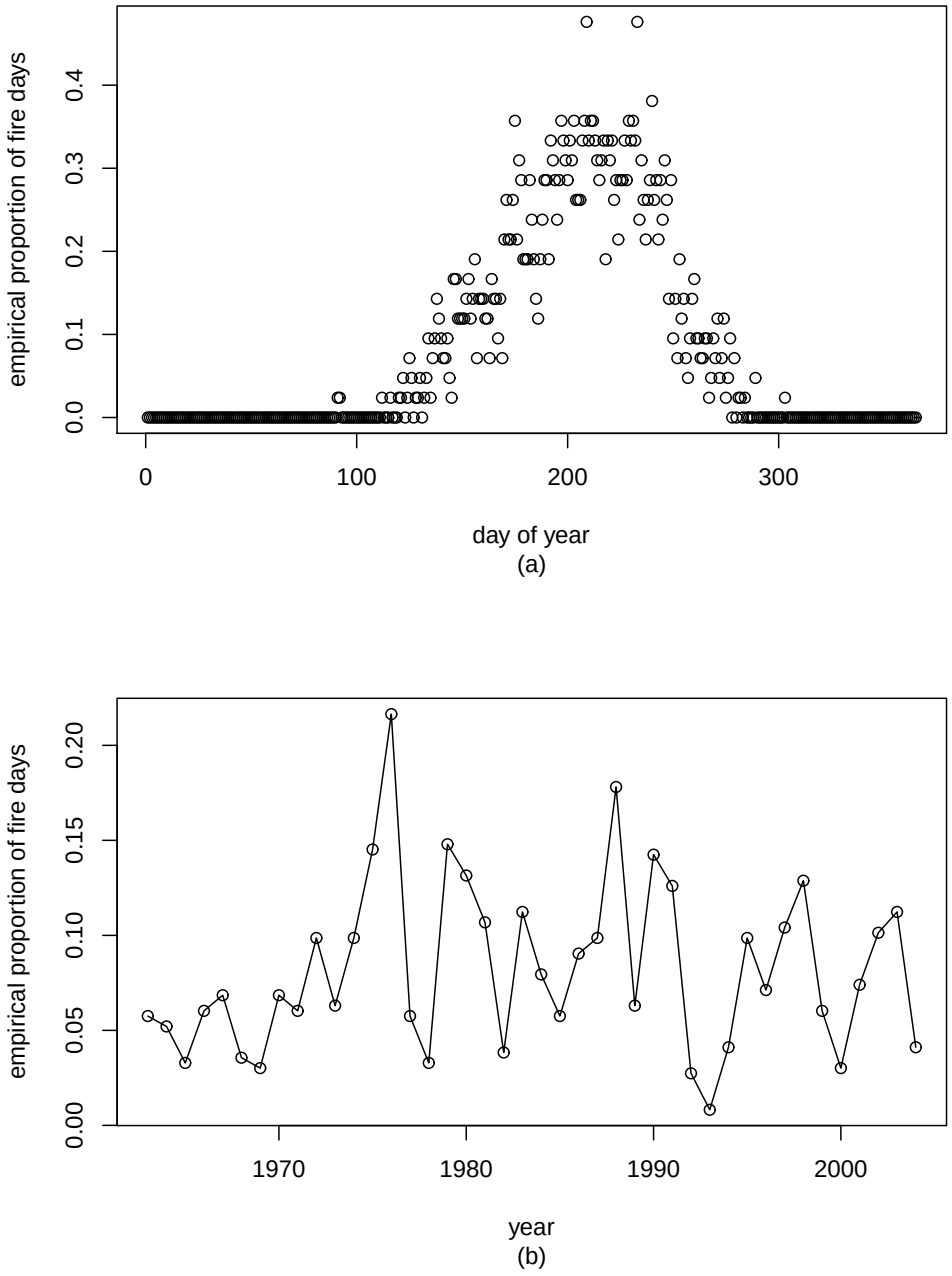

Figure 1: Observed empirical rates of fire days by day of year (panel a) and year (panel b).

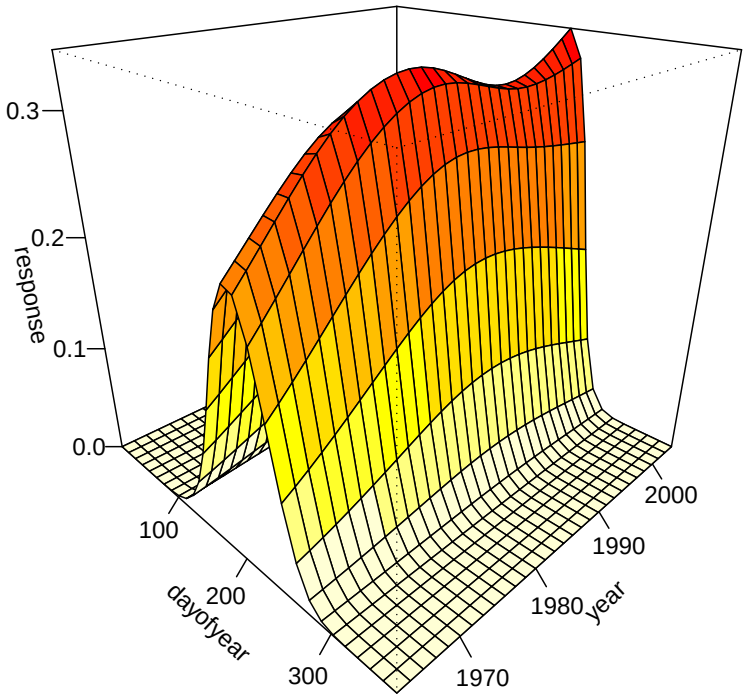

Figure 2: Visualization of the fitted probabilities from the model against day of year and year.

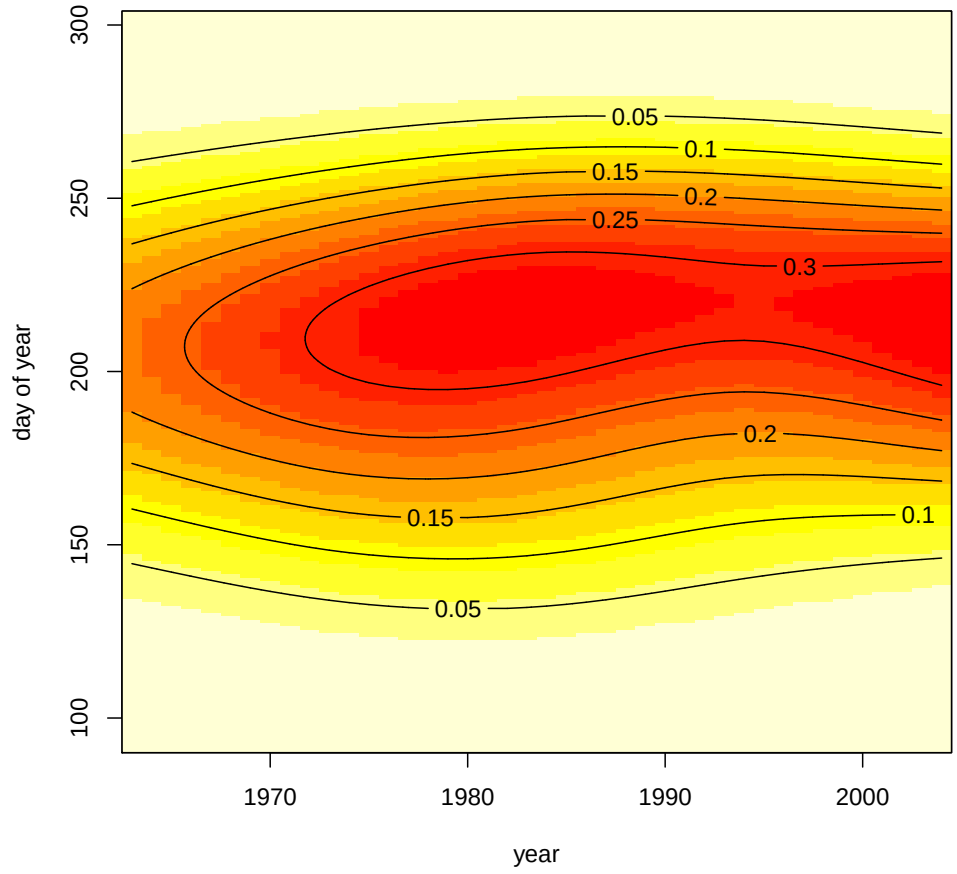

Figure 3: Contours of the fitted probabilities for Ontario's official "fire season" (April 1 through October 31) across years. Pixelated shading is used to emphasize the changes in the contours, where light yellow through dark red shading represents lower probability through higher probability, respectively.

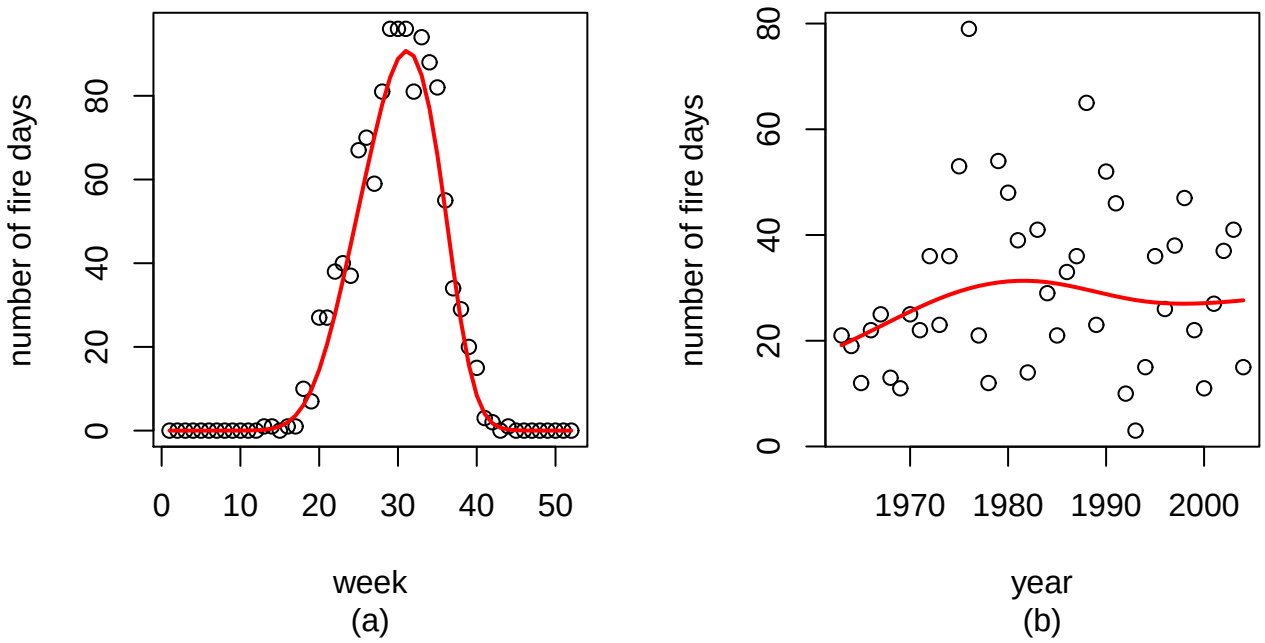

Figure 4: Observed (points) versus expected (line) aggregated by fortnight (panel a) and year (panel b).

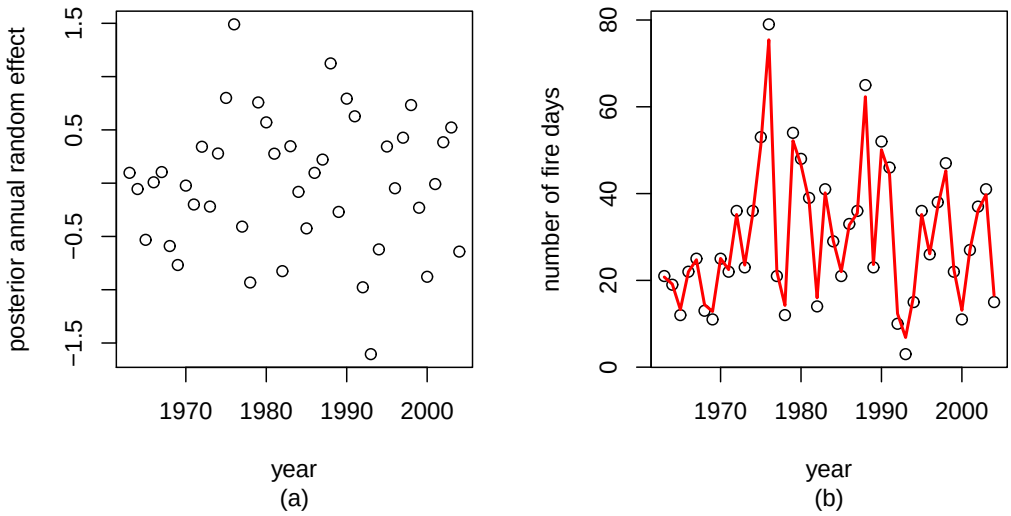

Figure 5: Panel (a): Posterior estimates of the annual random effects. Panel (b): Observed (points) versus expected (line) by year, incorporating the the posterior estimate of the annual random effect into the estimate.

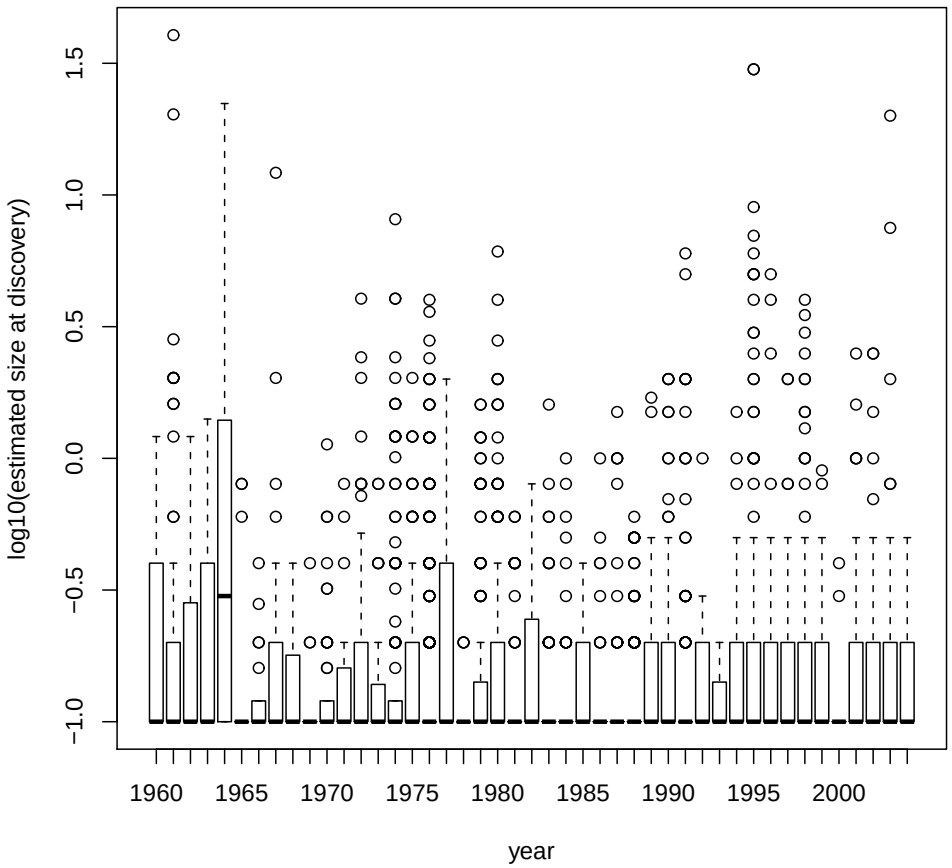

Figure 6: Annual boxplots of the $\log_{10}$ estimated discovery size for all lightning caused fires in the study region.